Chapter – 2

Experimental Procedure

2.1 Material

In this thesis experimental work was carried out on Ti+Nb stabilized IF steel of chemical composition C-0.0038%, Mn-0.5%, Si-0.008%, S-0.007%, P-0.036%, Ti-0.057%, Nb-0.016%, Al-0.031% (all by wt%) and balance Fe. The hot rolled plate of 440 x 350 x 30 mm^3 dimensions was obtained from M/S TATA steel Ltd, Jamshedpur.

2.2 Equal-Channel Angular Pressing

The steel billets of 15 mm diameter and 80 mm length were prepared from above hot rolled (followed by air cooling) plate of 440mm x 350mm x 30mm thickness in rolling direction. The samples were deformed at room temperature by equal-channel angular pressing (ECAP) using a hydraulic press of 30 ton adopting the route Bc [Furukwa et al. 1998] where samples were rotated by 90° always in one direction with respect to sample axis between two subsequent passes. Figure 2.1(a) shows the photograph of hydraulic press.

The sample surface was coated with a lubricant mixture of high density paraffin with MoS_2 to reduce friction between the billet and the die. The ECAP die used in the present investigation consists of two channels of 15 mm diameter each that intersect at an inner intersection angle Φ (120°) and an outer arc angle of Ψ (60°). The equivalent strain (ε_{vm}) was calculated using equation 1.7. The die of ECAP process was made up of die steel H11, of hardness ~ HRC 55. The above die introduces an equivalent strain (ε_{vm}) of ~0.6 during every passage of billet (Figure 2.1(b)). There was no back pressure applied

during ECAP process. The exit channel was 0.2 mm lesser than the inlet channel. The swelling was accommodated by this. The sample bars (die joining marks) were cleaned by papers. Loss in length was negligible. The billets were deformed to the maximum equivalent strain (ε_{vm}) of 24 (40 passes). About 20 mm lengths from both the ends of the ECAPed billet were removed to eliminate end effect.

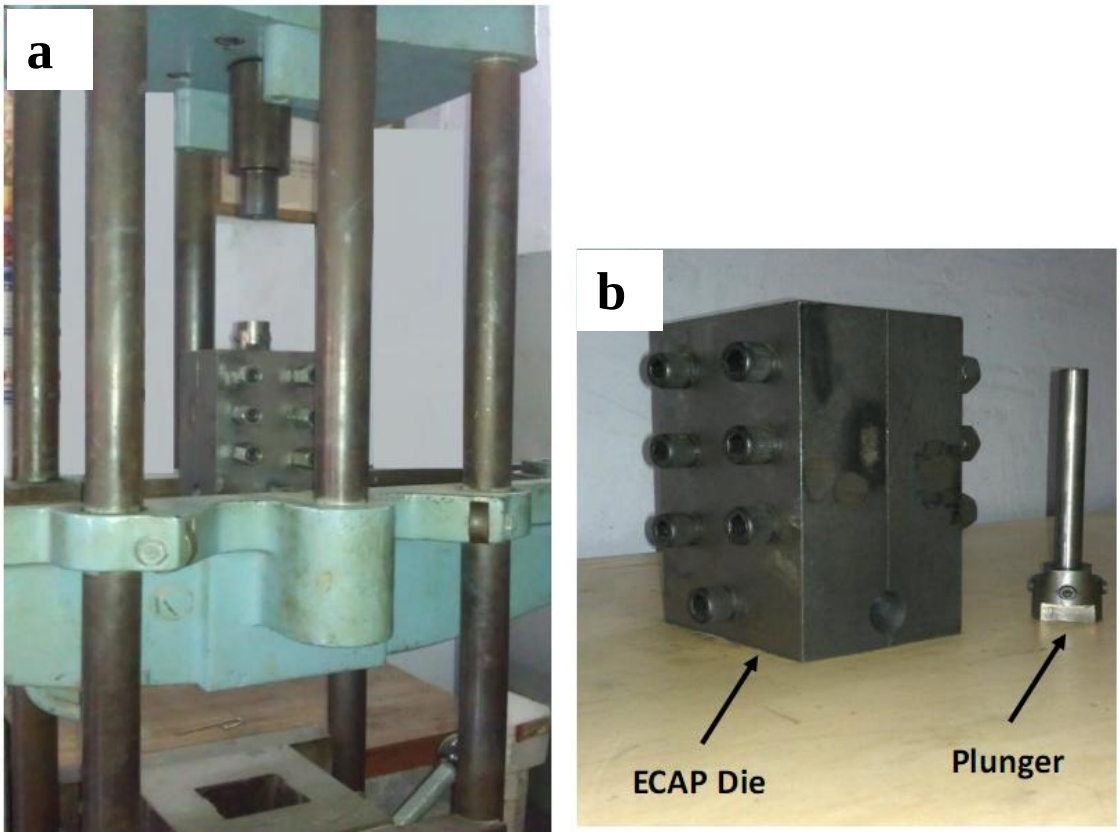

Figure 2.1: (a) Universal testing machine used in ECAP (b) ECAP die and plunger.

Figure 2.2(a) shows the section of die assembly with intersection angle φ=120º, ψ=60º, billet, shear plane and X, Y, Z directions. X plane was the transverse plane perpendicular to extrusion direction. Y plane was the flow plane vertical to the extruded billet and Z plane was the horizontal but parallel to top surface along extrusion direction. X direction is the extrusion direction, Y direction is the transverse direction and Z direction is normal direction. Therefore, ECAPed material Y plane is the ND-ED plane.

The major deformations take place on flow plane (ND-ED plane). Therefore, the chopped deformed samples were sectioned along Y plane for microstructural investigation.

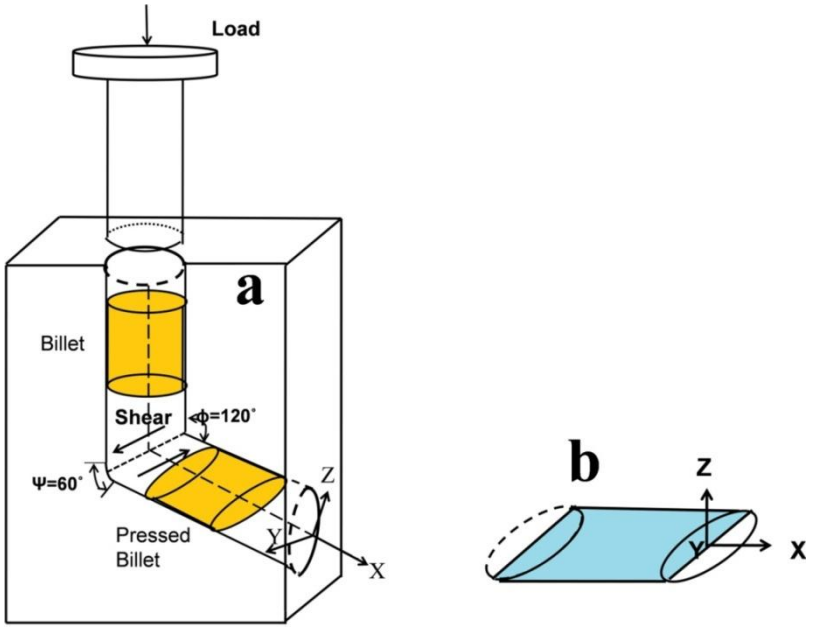

Figure 2.2: (a) Section of die assembly with intersection angles φ and ψ, billet, shear plane and X, Y, Z directions, b) Pressed Billet where the flow plane, Y plane is shown as colored plane with respect to X, Y, Z directions.

The ECAPed IF steel samples are denoted by ECAP-ε_{vm}. Where ε_{vm} indicates that the sample has undergone deformation by ECAP for equivalent Von Mises' strain of ε_{vm}. The designation of ECAPed samples are given in Table 2.1.

Table 2.1: Designations adopted for as-received and ECAPed IF steel samples.

S. No.	Details of sample	Designation
1	As-received	ECAP-0
2	ECAP for 1 pass	ECAP-0.6
3	ECAP for 2 pass	ECAP-1.2
4	ECAP for 3 pass	ECAP-1.8
5	ECAP for 4 pass	ECAP-2.4
6	ECAP for 5 pass	ECAP-3
7	ECAP for 10 pass	ECAP-6
8	ECAP for 15 pass	ECAP-9
10	ECAP for 20 pass	ECAP-12
11	ECAP for 25 pass	ECAP-15
12	ECAP for 30 pass	ECAP-18
13	ECAP for 35 pass	ECAP-21
14	ECAP for 40 pass	ECAP-24

2.3 Coldrolling and Cryorolling

ECAP-12) billets were machined to 61 X 13 X 7 mm^3 plate and subsequently coldrolled and cryorolled (on Z plane of ECAPed billet) to study the effect of temperature on deformation state of material. The plate samples were coldrolled to 90% reduction in area (designated as ECAP-12-CR-90) at room temperature. ECAPed plate samples were also cryorolled at 223K (-50°C) along their extrusion direction to the reduction in areas of 70 (designated as ECAP-12-CRR-70) and 96% (designated as ECAP-12-CRR-96). The required temperature for cryorolling was constantly maintained by mixing liquid nitrogen and ethanol and temperature was constantly monitored by calibrated Fe-constantan thermocouple. The designation of coldrolled and cryorolled samples is given in Table 2.2.

Table 2.2: Designation of ECAP followed by coldrolled and cryorolled IF steel samples.

S. No.	Details of sample	Designation
1	ECAP upto ε_{vm}=12 and Coldrolled for 90% reduction in area	ECAP-12-CR-90
2	ECAP upto ε_{vm}=12 and Cryo rolled for 70% reduction in area	ECAP-12-CRR-70
3	ECAP upto ε_{vm}=12 and Cryo rolled for 96% reduction in area	ECAP-12-CRR-96

2.4 Flash Annealing

ECAP-3, ECAP-12 and ECAP-21 samples were flash annealed at 823-1023K (550-750°C) in molten $NaNo_3$ salt for 5 minutes. The flash annealed samples were designated as ECAP-3-FAT, ECAP-12-FAT and ECAP-21-FAT. Where T indicates the temperature of flash annealing in °C. Temperature of salt bath was measured by chromel alumel thermocouple. Salt was put in a stainless steel container and the vessel was kept inside pit furnace. Temperature of salt bath was maintained by electric heating of pit furnace. Selective samples were annealed directly in electric furnace for flash annealing above 973K (700°C). A plunger was used to dip the sample in the melt. Then annealed samples were quenched in water at the end of soaking period. Designations of flash annealed samples are shown in Table 2.3.

Table 2.3: Designation of flash annealed IF steel samples.

S. No.	Details of sample	Designation
1	ECAP upto ε_{vm}=3 and flash annealed at 550˚C	ECAP-3-FA550
2	ECAP upto ε_{vm}=3 and flash annealed at 600˚C	ECAP-3-FA600
3	ECAP upto ε_{vm}=3 and flash annealed at 650˚C	ECAP-3-FA650
4	ECAP upto ε_{vm}=3 and flash annealed at 675˚C	ECAP-3-FA675
5	ECAP upto ε_{vm}=3 and flash annealed at 700˚C	ECAP-3-FA700
6	ECAP upto ε_{vm}=3 and flash annealed at 725˚C	ECAP-3-FA725
7	ECAP upto ε_{vm}=3 and flash annealed at 750˚C	ECAP-3-FA750
8	ECAP upto ε_{vm}=12 and flash annealed at 600˚C	ECAP-12-FA600
11	ECAP upto ε_{vm}=12 and flash annealed at 625˚C	ECAP-12-FA625
12	ECAP upto ε_{vm}=21 and flash annealed at 650˚C	ECAP-12-FA650
13	ECAP upto ε_{vm}=21 and flash annealed at 675˚C	ECAP-12-FA675
14	ECAP upto ε_{vm}=21 and flash annealed at 600	ECAP-21-FA600
15	ECAP upto ε_{vm}=21 and flash annealed at 625	ECAP-21-FA625
16	ECAP upto ε_{vm}=21 and flash annealed at (c) 675	ECAP-21-FA675
17	ECAP upto ε_{vm}=21 and flash annealed at 700°C	ECAP-21-FA700
18	ECAP upto ε_{vm}=12+Cold rolled for 90% reduction in area and flash annealed at 650˚C	ECAP-12-CR-90-FA650
19	ECAP upto ε_{vm}=12+Cold rolled for 90% reduction in area and flash annealed at 675˚C	ECAP-12-CR-90-FA675
20	ECAP upto ε_{vm}=12+Cold rolled for 90% reduction in area and flash annealed at 700˚C	ECAP-12-CR-90-FA700
21	ECAP upto ε_{vm}=12+Cryo rolled for 96% reduction in area and flash annealed at 550˚C	ECAP-12-CRR-96-FA550
22	ECAP upto ε_{vm}=12+Cryo rolled for 96% reduction in area and flash annealed at 600˚C	ECAP-12-CRR-96-FA600
23	ECAP upto ε_{vm}=12+Cryo rolled for 96% reduction in area and flash annealed at 675˚C	ECAP-12-CRR-96-FA675

2.5 Characterization of Ultrafine-grained IF Steel

IF steel samples were characterized for microstructure by optical microscopy (OM), scanning electron microscopy (SEM), electron back scattered diffraction (EBSD) and transmission electron microscopy (TEM). Bulk texture was studied by X-ray diffraction and mechanical properties were evaluated by hardness measurements and tensile testing. Fractured surfaces were investigated by scanning electron microscopy.

2.5.1 Microstructure

a. Optical Microscopy (OM)

Samples were cut from extrusion plane of ECAPed billet as well as from rolled sheets and polished for metallography by emery papers and cloths. Alumina abrasive was used for polishing and then polished samples were etched by 2% nital solution at room temperature. Microstructure of RD-TD surface or X-Y plane of coarse grained as-received IF steel and of ND-ED plane or Y plane from 0.6 to 1.8 of ECAP samples were examined using Metalux-3 optical microscope for determining grain size, grain shape, size and shape of deformation bands. Grain size of as-received material was measured on micrograph by Heyn's Lineal Intercept method. Band width of ECAP-0.6, ECAP-1.2, ECAP-1.8 was reported as grain size.

b. Scanning Electron Microscopy (SEM)

Microstructure of flash annealed samples of ECAP-3, ECAP-12, ECAP-21, ECAP-12-CR-90, ECAP-12-CRR-70 and ECAP-12-CRR-96 were investigated using Quanta 200 FEG SEM since the grain size of these samples is too small to be resolved by OM. Fracture surfaces of tensile tested samples were also investigated by SEM. ND-ED surfaces of ECAPed samples but RD-TD planes of rolled samples were viewed in SEM. Selective flash annealed samples were also mechanically polishing followed by electro polished at 283K (10°C), 16 V for 40 sec for observing microstructure.

c. Electron Back Scattered Diffraction (**EBSD**)

Electron back scattered diffraction (EBSD) is a technique to get crystallographic orientation, to identify crystal orientation mapping, microstructural heterogeneity investigations and to reveal microtexture or preferred orientation of any polycrystalline

material. ECAP-0-24, ECAP-12-CR-90, ECAP-12-CRR-70 and ECAP-12-CRR-96 and few selected samples of ECAP-12-CR-90-FAT, ECAP-12-CRR-70-FAT and ECAP-12-CRR-96-FAT were analyzed by EBSD. IF steel samples of dimensions 15 x 10 x 5.5 mm^3 were cut from the centre of the billet along flow plane (Y plane) and samples of 10 x 10 mm^2 were cut from rolled sheets. These were mechanically polished and were finally electropolished at 10°C, 16 V for 40 sec. The EBSD patterns of the electropolished samples were recorded from the ND-ED plane of ECAPed sample and RD-TD plane of rolled samples. The operating parameters of the microscope are set at the following: 20 kV excitation voltage, probe current 16-23 nA, working distance-16 mm, typical map size 0.87 mm^2 to 12100 μm^2 or 1.15 million points for ε_{vm}=0-1.2 and 1600 μm^2 at 2000X or 0.74 million points for ε_{vm}=1.8-24, step size of 0.1 μm for ε_{vm}=0-1.2 and 0.05 μm for εvm=1.8-2.4 and indexing rate of 154 fps. The coldrolled, cryorolled and flash annealed samples were scanned at step size of 0.05 μm at 16 mm working distance for area of 1600 μm^2 at 2000X. Misorientation angle and number fractions are analyzed using TSL (Texture Scanning Electron Microscope Lab) 5.1 software. Scanned data were analysed for misorientation angle, high angle and low angle grain boundary fraction. Image quality maps are included on which low angle grain boundaries (LAGBs) of misorientation angle (2-15º) and high angle grain boundaries (HAGBs) of misorientation angle of 15-62.8º are delineated by red color and blue color lines respectively. Characterization procedure for microtexture is reported after bulk texture. The magnified view of selected area is given at left hand top corner of the map to show the boundary distribution on the corresponding figure as an inset some the selected equivalent strains. Grain size was also analysed from scan data using the software.

d. X-Ray Diffraction (XRD)

ECAP-0 to ECAP-24 IF steel samples were scanned by Cu Kα radiation (λ=1.54 nm) radiation using a Bruker D8 Discover diffractometer. Samples were illuminated by 1 mm diameter X-ray beam with 2Θ range of 25-135° and step size of 0.05°. The instrument was calibrated for instrumental broadening. Well annealed, as-received and rolled samples were scanned on RD-ND plane but ECAPed samples were scanned on ND-ED plane. The elastic stored energy (E_l) in (112) plane was calculated with the help of equation (2.1) derived by G. R. Stibitz [Stibitz et al. 1936, Hazra, Gazder, Pereloma et al. 2009]

$$E_l = \frac{3}{2} Y \frac{\left(\frac{\delta d}{d}\right)^2}{1+2\nu^2} \quad (2.1)$$

Where, δd/d is the lattice strain (variation in interplanar spacing) which is calculated by following equation

$$\frac{\delta d}{d} = \frac{\beta}{2tan\theta} \quad (2.2)$$

Here, β is full width at half maximum of the X-ray peak profile, 2θ is the Bragg's angle, Y is the directionally dependent Young's modulus and ν is Poisson's ratio. The Young's modulus for 110 direction, Poisson's ratio and molar volume of iron were taken as 221 GPa, 0.3 and 7.11 cc/mole respectively [Borbely et al. 2000]. Full width at half maxima (β) is determined from X'Pert high software by fitting the line profiles with a pseudo-Voigt function. Goodness of fit was 0.997. Illumination size of 1mm diameter, 2Θ range of 25-135º and step size of 0.05º are used.

A well annealed IF steel, as-received IF steel and ECAP-12, ECAP-12-CR-90, ECAP-CRR-70 and ECAP-12-CRR-96 and their flash annealed samples of ECAP+cold

rolled as well as cryorolled samples were scanned. Well annealed sample, as-received and rolled samples were scanned on RD-TD plane but ECAPed samples were scanned on ND-RD plane. The samples are scanned by a Rigaku Mini Flex 600 system using Cu Kα radiation (λ=0.154 nm) operating at 40kV voltage and 15mA current. Integral breadth for (112) plane is determined by fitting line profiles with Gaussian and Lorentzian functions. Goodness of fit is 0.997. Intensity for all samples is measured by varying 2Θ from 42° to 143° with a step size of 0.02° and a scan rate 4°/min.

The elastic stored energy (E_l) in (112) plane was calculated from X-Ray diffraction measurement using an equation (1) derived by G. R. Stibitz [Stibitz 1936, Hazra et al. 2009]

$$E_l = \frac{3}{2} Y \frac{\left(\frac{\delta d}{d}\right)^2}{1+2\nu^2} \tag{2.3}$$

Where δd/d is ratio of change in interplanar spacing with interplanar spacing and can be calculated by

$$\frac{\delta d}{d} = \frac{\sqrt{\beta^2 - \beta_0^2}}{2tan\theta} \tag{2.4}$$

Here β is full width at half maximum (FWHM) and β_0 is FWHM of well annealed material, Y and ν are the Young's Modulus and Poisson's ratio respectively. Young's Modulus for [112] directions is 221 GPa [Borbely et al. 2000]. Poisson's ratio was taken as 0.3 and molar volume of iron 7.11 cc/mole.

The corrected Lorentzian (L) component of the integral breadth β'_L was separated from instrumental breadth using following relation

$$\beta'_L = \beta_L - \beta_{L0} \tag{2.5}$$

Where β_{L0} is the Laurentzian component of integral breadth of well annealed material. β_L is Laurentzian component of integral breadth. The corrected (from instrumental broadening) Gaussian component (β'_G) of integral breadth value was extracted from the Gaussian component (β_G) using the following equation

$$\beta'^2_G = \beta^2_G - \beta^2_{G0} \quad (2.6)$$

β_{G0} is the Gaussian component of integral breadths of well annealed material.

The volume average domain size (D) and lattice strain were calculated from the following relationship [Klug et al. 1954]

$$D = \lambda/\beta'_L \cos\theta \quad (2.7)$$

$$e = \frac{\beta'_G}{4\tan\theta} \quad (2.8)$$

Where θ is the Bragg angle, D is average domain size, λ is wavelength of the X-ray radiation. The calculated strain value was multiplied by 100 for percentage strain. Integral breadth for (112) plane was determined by fitting line profiles with Gaussian and Lorentzian functions. The diffraction patterns are given in appendix (A-Figure 1 (a-m) and 2 (a-c)).

e. Bulk Texture

ECAP-0.6 toECAP-24 were scanned for bulk texture measurement on the Y-plane but ECAP-0, ECAP-12-CR-90, ECAP-CRR-70 and ECAP-12-CRR-96 i.e. rolled samples were scanned on RD-TD plane. Texture was determined by X-ray diffraction with a PANalytical X'Pert PRO MPD system using Cu Kα radiation obtained at the acceleration voltage of 45 kV and current 40 mA. The texture was represented by pole figures and orientation distribution functions (ODFs). The orientation distribution functions (ODFs)

were obtained by the inversion of 4 incomplete pole figures [(100), (110), (112) and (103)] using the MTM-FHM software [Houtte 2009]. All the pole figures and ODFs were analysed based on main ideal orientations in simple shear deformation of BCC materials [Li et al. 2005].

Pole Figure

A pole figure is a stereogram with its axes defined by an external frame of reference with particular *hkl* poles plotted onto it from all of the crystallites in the polycrystal. Typically, the external frame is defined by the ND, RD and TD in a sheet respectively. If the material shows a degree of texture, the resultant pole figure will show the accumulation of poles about specific directions. A single crystal can be plotted on the pole figure and there is no ambiguity regarding its orientation. However as more crystallite poles are plotted onto the pole figure the specific orientation of a particular crystallite can no longer be defined. For a large number of grains in a polycrystal poles may overlap on the pole figure so that the true orientation density is not clearly represented. In this case contours tend to be used instead. Regions of high pole density have a high number of contours while regions with low pole density have a few greatly spaced contours. Figure 2.3 shows a (110) pole with contour density. The ECAE simple shear model textures depict partial <111>-fiber that are counter clock wise rotated around TD for $\theta \sim 60°$ for $\Phi \sim 120°$ die (Figure 2.3) from those associated with negative simple shear [Li et al. 2005]. All the pole figures were analysed based on main ideal orientations in simple shear deformation of BCC materials [Li et al. 2005]. The {110} pole figures were in TD view for ECAP process accompanied by rotation of billet of $\theta \sim 60°$ around TD for negative simple shear.

Here SD stands for shear direction, SPN for shear plane normal, ED for extrusion direction and ND for normal direction. In the present investigation (110) pole figures with orientation density contour levels of 0.8,1,1.3,1.6,2,2.5,3.2,4,5,6.4. Pole figures do not display all texture components, so a combination of pole figures is required to represent texture completely. There is need for an alternative representation of texture. The axis of pole figures of ECAP-ε and rolled samples/as-received material (ECAP-0) are represented as ND view in Figure 2.3a and Figure 2.3b respectively.

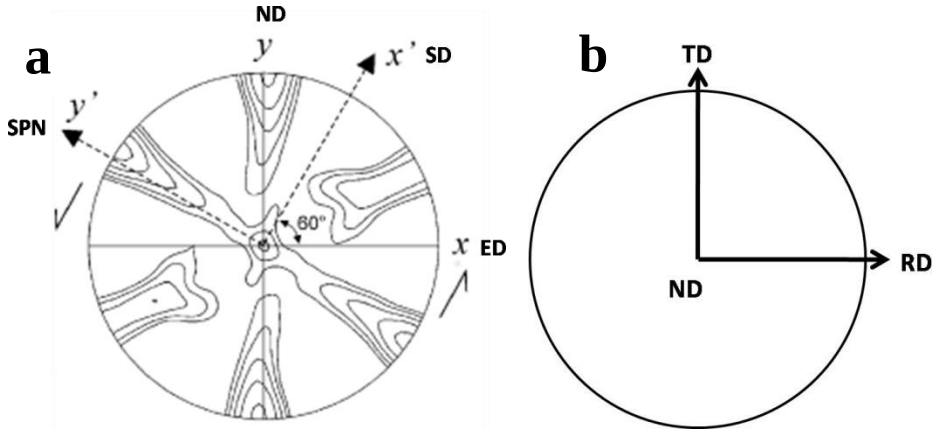

Figure 2.3: (a) (110) pole figure showing the ideal ECAE texture simulated by the Taylor model for bcc materials after one ECAE pass with Φ=120°, (b) directions of rolled samples.

Orientation distribution function (ODF)

Orientation distribution function (ODF) describes the distribution of orientation in orientation space (called Euler's space). In Euler's space orientation of a crystal is represented by three Euler angles φ_1, Φ, φ_2. The Euler angles refer to three rotations that transform the specimen coordinate system into the crystal coordinate system or denote the orientation g [Engler et al. 2010] (Fig. 2.4). There are several different conventions for expressing the Euler angles. Bunge, conventions are used [Bunge, 1965, 1982] in the thesis. In the present investigation X [100], Y[010] and Z[001] are three crystallographic

directions and A, B and C are the three deformation directions RD, ND and TD respectively. Then, φ1 is rotation angle of crystal around Z till X is parallel to AB, Φ is rotation angle of crystal around X till Z is parallel to C and φ_2 is rotation angle of crystal around Z such that X is parallel to A, Y is parallel to B and Z is parallel to C.

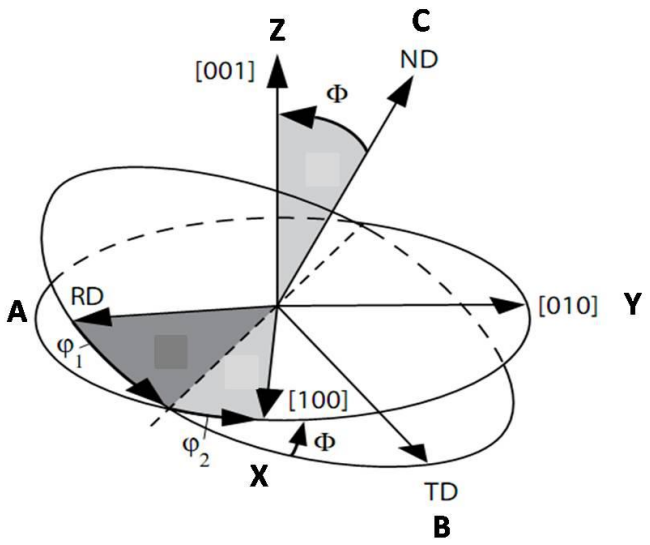

Figure 2.4: Schematic representation of Euler angles φ_1, Φ, and φ_2 [Engler et al. 2010].

Any point in this space corresponds to a single orientation (hkl)[uvw] and the density at that point is the strength of that orientation (texture component) in x-random unit. The volume of orientation space is divided by contour surfaces which separates region of higher and lower orientation density. Since it is difficult to handle such a three dimensional plot the final representation is usually made as a series of parallel sections through this space usually along φ_2. A series of sections along φ_2 (usually at fixed interval of angle) are arranged sequentially in two dimensional plane as 2D plots of ODF maps (φ vs φ_1 for a given φ_2) where every point represents an orientation (hkl)[uvw] with orientation density contours.

The ODF is defined as distribution in the volume fraction of grains having orientation g with variation in orientation

$$ODF\ (g) = \frac{1}{V}\frac{dV(g)}{dg} \qquad (2.9)$$

Where, V is the total volume and dV(g) is the volume with orientation g represented by the Euler angles φ_1, φ and φ_2. dV(g)/dg is the change in orientation volume with change in orientation.

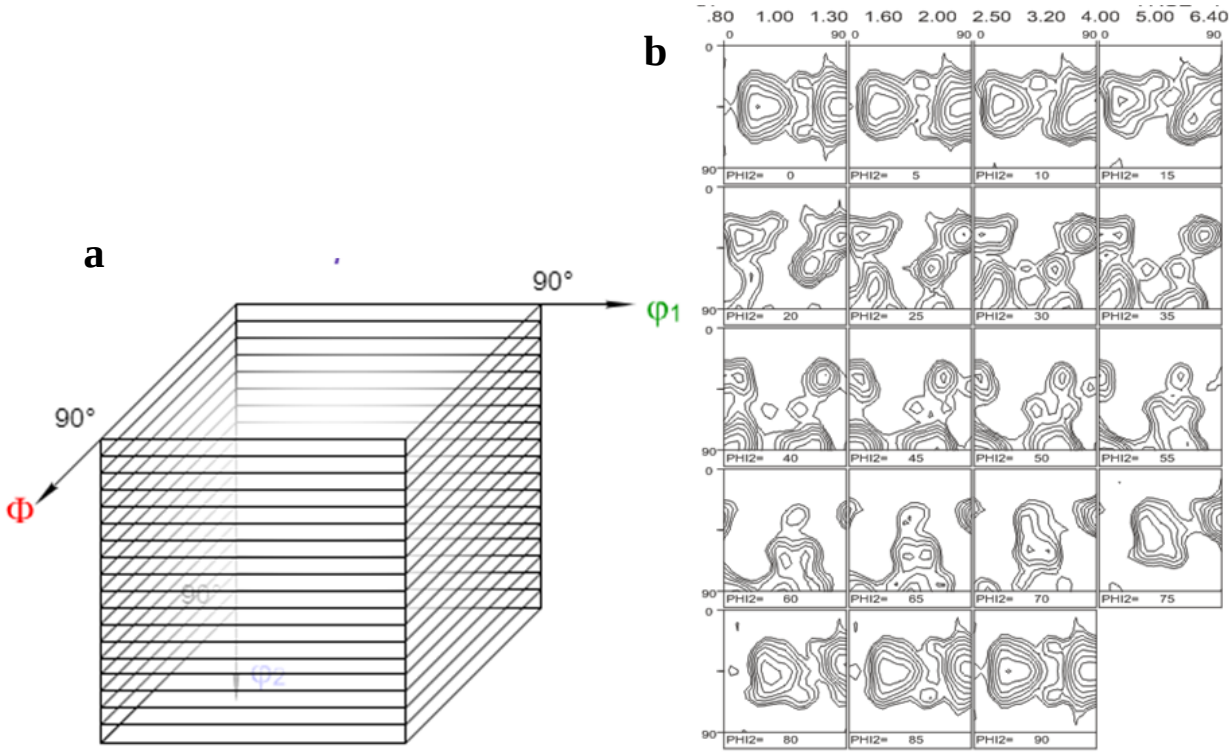

Figure 2.5: (a) Orientation space is divided into slices at φ_2=5° intervals and (b) 2D-Typical orientation distribution Function (ODF) maps.

In general the angles range over $0° \leq \varphi_1 \leq 360°$; $0° \leq \Phi \leq 180°$; $0° \leq \varphi_2 \leq 360°$. In shear texture representation of ECAPed IF steel, $0° \leq \varphi_1 \leq 360°$; $0° \leq \Phi \leq 90°$; for φ_2=0 and 45° are reported in the present study with ODF intensity contours of 0.8,1.2,2,3,5,7.5,10,13,17,22. The main ideal orientations and fiber textures in simple

shear of bcc materials are listed in Table 1.1 [Li et al. 2005]. The orientation distribution functions (ODFs) were obtained by the inversion of 4 incomplete pole figures [(100), (110), (112) and (103)] using the MTM-FHM software [Houtte 2009]. However for rolled IF steel, ODFs, $0°\leq\varphi_1\leq90°$; $0°\leq\Phi\leq90°$; for $\varphi_2= 45°$ are displayed with ODF intensity contours of 0.8, 1, 1.3, 1.6, 2, 2.5, 3.2, 4, 5, 6.4.

Inverse Pole Figure

An inverse pole figure shows position of a sample direction relative to crystal reference frame. Instead of plotting crystal orientations with respect to an external frame of reference, inverse pole figures can be produced which show the RD, TD and ND respectively with respect to the crystallographic axes. This figure uses a crystallographic unit triangle as a reference frame with contour lines to show the frequency with which various directions in the crystal coincides with the specimen axis under consideration. Therefore, they are also called axis distribution charts. In the present report [001] inverse pole figures were generated and reported. Figure 2.6 (a1) gives the color codes for inverse pole figure [001] and Figure 2.6 (a2) displays sample directions for rolled or as-received material. Figure 2.6 (a3) gives directions for ECAPed samples on Y-plane. This indicates that transverse direction is parallel to crystallographic axis of Figure (2.6a3) but in case of rolled samples (i.e. as-received and cold rolled and cryorolled samples) normal direction is parallel to crystallographic direction of Figure 2.6 (a2).

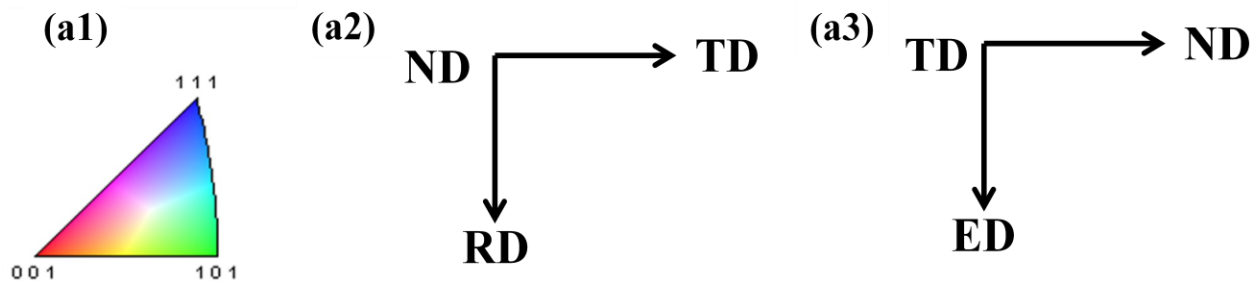

Figure 2.6: (a1) Color codes for inverse pole figure [001], (a2) directions of rolled samples, (a3) directions of ECAPed sample on Y-plane, ED=extrusion direction (X direction), ND=normal direction (Y direction), TD=transverse direction (Z direction).

f. Micro Texture

EBSD scanned data for microtexture were analyzed using TSL (Texture SEM Lab) 5.1 software and (110) pole figures were reported with contour levels of 0.788, 1, 1.149, 1.517, 1.743, 2.003, 2.301, 2.644.

g. Transmission Electron Microscopy (TEM)

Thin slices of 0.2-0.5 mm were cut from ECAP-0 to ECAP-24, ECAP-12-CR-90 and ECAP-12-CRR-70 and ECAP-12-CRR-96 samples as well as their flash annealed samples were analyzed by TEM measurement. The discs of 3 mm diameter 40 µm thickness were punched from the thin foil and electropolished at 243K (-30°C) using an electrolyte of 5 vol.% perchloric acid and 95 vol.% methanol at 30 V, ~60 mA. Electropolished samples were investigated by Tecnai $20G^2$ TEM working at 200kV. Y plane or ED-ND planes of ECAPed samples and RD-TD planes of as-received rolled as-well as rolled flash annealed samples were investigated. Microstructures were analyzed for structural homogeneity, morphology of bands as well as grains and cells, subgrains, grain size, grain orientations, distribution of dislocation density and nature of grain

boundary etc. the band width is represented as grain size for banded structure from TEM micrographs (ε_{vm}=1.2-12). Each band/grain/cell/subgrain is measured individually from five micrographs. While bands are not visible in the samples for ε_{vm}=15-24 grain/subgrains are considered as grains and their average size is reported as grain size.

2.6.2 Mechanical Properties

a. Hardness

Metallographic samples were investigated for hardness measurement. Hardness was measured by Shimadzu HMV-2T Microhardness tester at varying load of 10g to 2 kg to find out minimum load required for load independent hardness in Y plane of ECAPed sample and rolling plane of rolled samples. Load independent hardness was found to be at 980 mN therefore all measurements were done at minimum load of 980 mN. Average hardness value with standard deviation was reported for 10 measurements on each sample.

b. Tensile Test

Tensile tests were conducted on bar specimens along extrusion direction for ECAPed samples having the gauge length of 16 mm and gauge diameter of 4.5 mm (Figure 2.7). Plate samples of gauge length 15 mm, width 5 mm and thickness ~1mm were prepared from rolled sheets of ECAP-12-CR-90 and ECAP-12-CRR-70 and ECAP-12-CRR-96 as well as their flash annealed samples for tensile testing (Figure 2.8). Samples were tested on INSTRON model 4206 at room temperature at a constant cross head speed of 1 mm/min. 0.2 proof stress, ultimate tensile strength, uniform elongation and total elongation were calculated from load elongation plot. Because of large amount

of deformation, the number of sample to be prepared is large and time consuming, tensile data for only one sample for each strain level was reported and therefore no standard deviation value is available.

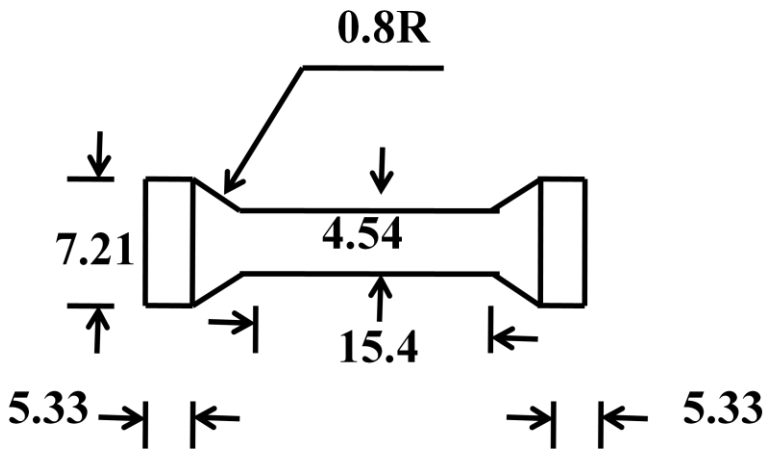

Figure 2.7: Dimensions of round tensile sample (all dimensions are in mm).

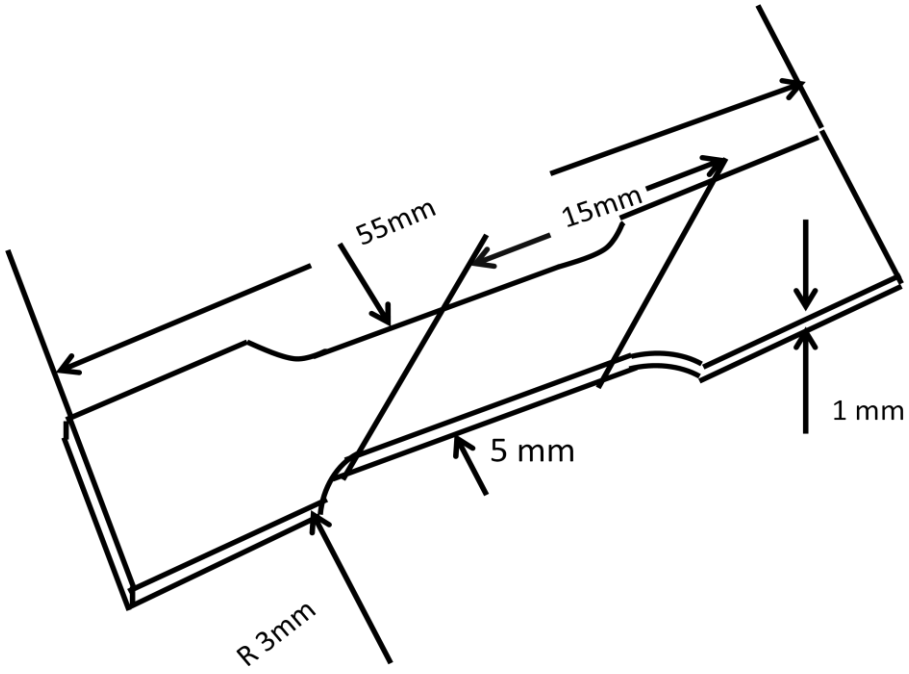

Figure 2.8: Dimensions of flat tensile sample.

c. Fractography

Fractured surfaces of ECAP-0 to ECAP-24, ECAP-12-CR-90 and ECAP-12-CRR-70 and ECAP-12-CRR-96 samples were investigated by Quanta 200 FEG SEM. Dimples/ductile fracture zones were labeled by D but for brittle or cleavage fracture regions were denoted by A. The diameters of large dimples were measured at 25 different locations of various micrographs and standard deviation value was reported. Comments on depth were made on visual observation. Correlations between the processing parameters, microstructure, texture and the mechanical properties were established.